Carbohydrate Polymers 90 (2012) 189–196

Contents lists available at SciVerse ScienceDirect

Carbohydrate Polymers

journal homepage: www.elsevier.com/locate/carbpol

Bioconjugation of quantum-dots with chitosan and *N*,*N*,*N*-trimethyl chitosan

Herman S. Mansur[a,*], Alexandra A.P. Mansur[a], Elisabete Curti[b], Mauro V. De Almeida[b]

[a] *Department of Metallurgical and Materials Engineering, Federal University of Minas Gerais, Av. Antônio Carlos, 6627 – Escola de Engenharia, Bloco 2 – Sala 2233, 31.270-901, Belo Horizonte, MG, Brazil*

[b] *Department of Chemistry, Federal University of Juiz de Fora, Campus Martelos, 36.036-330, Juiz de Fora, MG, Brazil*

ARTICLE INFO

Article history:
Received 7 March 2012
Received in revised form 1 May 2012
Accepted 5 May 2012
Available online 11 May 2012

Keywords:
Chitosan
Carbohydrates
Quantum dots
Biopolymer
Bioconjugates

ABSTRACT

Novel carbohydrate-based hybrids combining chitosan and chemically modified chitosan with CdS inorganic nanoparticles were designed and prepared via aqueous route at room temperature. *N*,*N*,*N*-trimethylchitosan (TM-chitosan) was synthesized aiming at substantially improving the water solubility of chitosan for producing stable colloidal systems. UV–vis spectroscopy, photoluminescence spectroscopy, Nuclear magnetic resonance spectroscopy, Raman spectroscopy, and Fourier transform infrared spectroscopy were used to characterize the synthesis and the relative stability of biopolymer-capped CdS nanocrystals. The results have clearly indicated that chitosan and chitosan-derivative (TM-chitosan) were remarkably effective on nucleating and stabilizing CdS nanoparticles in aqueous suspensions. In addition, the CdS nanocrystals were produced in the so-called "quantum-size confinement regime", with the calculated average size below 3.5 nm and fluorescent activity in the visible range of the spectra. Therefore, a new single-step process was developed for the bioconjugation of quantum dots with water soluble chemically functionalized carbohydrates at room temperature for potential biomedical applications.

1. Introduction

Chitosan (poly-β(1→4)-2-amino-2-deoxy-D-glucose) is one of the most abundant polysaccharide in nature. It is produced by alkaline deacetylation of the natural polymer chitin mostly extracted from crab and prawn shells. Essentially, chitosan is a copolymer composed of *N*-acetyl-D-glucosamine and D-glucosamine units available in different grades depending upon the degree of acetylated moieties. It is a polycationic complex carbohydrate that has one amino group and two hydroxyl groups in the repeating glucosidic residue (Costa-Júnior, Barbosa-Stancioli, Mansur, Vasconcelos, & Mansur, 2009). Carbohydrate based polymers provide the chemist with a broad spectrum of raw materials for biomedical applications that exhibit biodegradability and biocompatibility. In the last 2 decades, it has become increasingly important due to its versatile potential use in many scientific and industrial fields like food conservation and drug delivery (Costa-Júnior et al., 2009; Dash, Chiellini, Ottenbrite, & Chiellini, 2011; Muzzarelli et al., 2012; Rinaudo, 2006). In that sense, the chemical modification of the chitosan comes as a promising strategy to be followed considering a much broader use as biomaterials, tissue engineering, cell targeting, and imaging, among others (Costa-Júnior et al., 2009; Dutta, Dutta, & Tripathi, 2004; Muzzarelli, 2009; Muzzarelli, 2011). A new area of research in nanotechnology is getting increasing attention focusing on the development of hybrids nanomaterials based on biocompatible polymers, especially by combining organic and inorganic nanoparticles with proteins and carbohydrates in a myriad of novel applications (Mansur & Mansur, 2011; Mansur & Mansur, 2012; Mansur A, Mansur, & González, 2011; Mansur, H. S., Mansur, & González, 2011a; Mansur, H. S., Mansur, & González, 2011b).

The semiconductor nanocrystals, often referred as "quantum dots" (QDs), are one of the most exciting fields in nano-science of the current century, basically because of the drastic changes in most properties of materials as a result of the direct influence of the ultra-small length scale on the energy band distribution (Brus, 1984; Li, Zhong, Zhou, Yang, & Li, 2006; Mansur, Grieser, Urquhart, & Furlong, 1995b; Mansur et al., 1995a; Mansur, Vasconcelos, Grieser, & Caruso, 1999; Mansur, 2010; Medintz, Uyeda, Goldman, & Mattoussi, 2005; Urquhart, Furlong, Mansur, Grieser, & Tanaka, 1994; Ye, Zhong, Zheng, Yang, & Li, 2007). These are promising nanomaterials concerning to the exploitation of their features in all areas of science, mainly those associated with biomedical applications such as nanobiotechnology and nanomedicine (Mansur, 2010; Medintz et al., 2005). In addition, to be used in biological environments they must exhibit compatibility to the physiological medium where water is abundant and with the large number of natural macromolecules such as carbohydrates, proteins, or synthetic ones, like polymers. Regardless the route one may choose, the whole system dimension must be kept within a very limited

* Corresponding author. Tel.: +55 31 34091843; fax: +55 31 34091843.
E-mail address: hmansur@demet.ufmg.br (H.S. Mansur).

0144-8617/$ – see front matter © 2012 Elsevier Ltd. All rights reserved.
http://dx.doi.org/10.1016/j.carbpol.2012.05.022

range as the "hydrodynamic diameter" will establish its behaviour in most biological applications (Mansur & Mansur, 2011; Mansur, A., et al., 2011; Mansur, H. S., et al., 2011a; Mansur, H. S., et al., 2011b). As a consequence, the development of innovative procedures for producing water soluble QDs, with long-time stability, narrow size distributions, and biocompatibility, associated with the least possible "hydrodynamic diameter" (i.e. size) has driven the research in this theme. Amongst several choices, biopolymers such as chitosan come as an interesting possibility of synthesizing semiconductor nanocrystals, as they share some of the major requirements for that purpose (Li, Du, Zhang, & Pang, 2003). Few reports have been published about combining quantum dots with chitosan but they have focused on films and nanoparticles of chitosan with embedded quantum dots in the polymer matrix (Jiang, Zhu, Yao, Fu, & Guan, 2012; Li et al., 2003).

Thus, to the best of our knowledge, the present study is the first report to investigate the synthesis and characterization of CdS quantum dots using both chitosan and chemically modified chitosan as "capping" ligands in aqueous solutions by one-step colloidal chemistry.

2. Materials and methods

2.1. Materials

All reagents and precursors, thioacetamide (Sigma–Aldrich, USA, ≥99%, CH_3CSNH_2), cadmium perchlorate hydrate (Aldrich, USA, $CdClO_4{\cdot}6H_2O$), sodium hydroxide (Merck, USA, ≥99%, NaOH), sodium sulphide (Synth, Brazil, >98% $Na_2S{\cdot}9H_2O$), acetic acid (Synth, Brazil, ≥99.7%, CH_3COOH), hydrochloric acid (Sigma–Aldrich, USA, 36.5–38.0%, HCl), methyl iodide (Sigma–Aldrich, USA, ≥99%, CH_3I), sodium iodide (Sigma–Aldrich, USA, ≥99%, NaI), *N*-methyl-2-pyrrolidone (VETEC, Brazil, ≥99%, C_5H_9NO), and ethanol (VETEC, Brazil, ≥95%, C_2H_6O) were used as-received. Chitosan powder (Aldrich Chemical, USA, medium molecular weight, M_W = 161,000 g/mol, degree of deacetylation, DD ≥ 75.0%, and viscosity 800–2000 cPoise, at 1% in 1% acetic acid) was used as the reference ligand. De-ionized water (DI-water, Millipore Simplicity™) with resistivity of 18 MΩ·cm was used in the preparation of all solutions.

2.2. Preparation methods of CdS precursor solutions

Approximately 0.0601 g CH_3CSNH_2 was added to 75 mL of DI-water in a 100 mL flask and homogenized under moderate manual stirring for 10–15 min at (23 ± 2) °C. Then, the volume was completed to 100 mL with DI-water. This sulphur precursor stock solution was referred as "SOL_S1".

Approximately 0.196 g of hydrated sodium sulphide was added to 75 mL of DI-water in a 100 mL flask and homogenized under moderate manual stirring for 10–15 min at (23 ± 2) °C. Then, the volume was completed to 100 mL with DI-water. This sulphur precursor stock solution was referred as "SOL_S2".

Approximately 0.4193 g of $Cd(ClO_4)_2{\cdot}6H_2O$ was added to 75 mL of DI-water in a 100 mL flask and homogenized under moderate manual stirring for 10–15 min at (23 ± 2) °C. Then, the volume was completed to 100 mL with DI-water. This cadmium precursor stock solution was referred as "SOL_Cd".

2.3. Preparation of reference chitosan (CHI) 1.0% (w/v) solution

Chitosan solution (1%, w/v) was prepared by dispersing chitosan (2.59 g) in a 250 mL aqueous solution (2%, v/v) of acetic acid. The solution was placed under constant stirring overnight at room temperature, until complete solubilization has occurred (pH ~ 3.6). The solution of chitosan was diluted for nanoparticle synthesis at 0.45 g·L^{-1} in water (referred as "SOL_CHI").

2.4. Procedure for preparation of trimethyl chitosan chloride (TM-chitosan)

To prepare *N*,*N*,*N*-trimethylchitosan (TM-chitosan), 1.0 g of chitosan was suspended in 40 mL of *N*-methyl-2-pyrrolidone and 5.5 mL of aqueous NaOH solution (20% m/v). Then, it was added 8 mL of methyl iodide and 2.4 g of sodium iodide. The reaction has occurred under moderate stirring for 48 h at room temperature. The product *N*,*N*,*N*-trimethylchitosan iodide (TM-chitosan-I) was collected by precipitation from solution using ethanol. After filtering, it was dried under vacuum (24 h) at room temperature resulting on approximately 2 g of *N*,*N*,*N*-trimethylchitosan iodide. To exchange the counter-ions iodide (I^-) by chloride (Cl^-), the intermediate obtained material (TM-chitosan-I) was re-dissolved in water and this solution was submitted to dialysis in a cellophane membrane (cut-off 12,000–14,000 g/mol) in the sequence: (a) against aqueous 0.2 M NaCl and (b) against water. The resulting solution was freeze-dried and TM-chitosan was retrieved as water-soluble white flakes (Curti, Britto, & Campana-Filho, 2003).

TM-chitosan solution for quantum dot synthesis (1.0%, w/v) was prepared by dissolving 0.1 g of TM-chitosan flakes in 10 mL of DI-water under moderate magnetic stirring for 30 min until complete solubilization has occurred (pH ~ 4.8). The solution of TM-chitosan was diluted for nanoparticle synthesis at 0.45 g L^{-1} in water (referred as "SOL_TMC").

2.5. Synthesis of CdS nanoparticles in chitosan and TM-chitosan solutions

CdS nanoparticles were synthesized via aqueous route in a reaction flask by using the stock solutions as detailed in the previous section, Cd^{2+} and sulphur precursors, and chitosan or TM-chitosan as capping ligands.

The thioacetamide is a sulphur precursor which on hydrolysis gives hydrogen sulphide being a useful substitute for H_2S gas. The stoichiometric equation (Eq. (1)) describes the complete hydrolysis reaction that occurs in two steps (Peeters & de Ranter, 1974; Rosenthal & Taylor, 1957).

$$CH_3C(S)NH_{2(aq)} + 2H_2O \rightarrow CH_3CO_2H + H_2S_{(g)} + NH_{3(aq)} \quad (1)$$

This reaction is catalyzed by both, acids and bases. The base-catalyzed reaction was found to be more rapid (Mansur, H. S., et al., 2011a; Rosenthal & Taylor, 1957). However as chitosan is not soluble in alkaline media, the thioacetamide hydrolysis in acid medium was attempted by reducing the pH of "SOL_CHI" to (0.5 ± 0.2), (1.5 ± 0.2) and (2.5 ± 0.2) through the addition of HCl 1.0 mol L^{-1}. Nevertheless the formation of CdS nanoparticles in these acid environments was not detected after 5 days. Thioacetamide choice as sulphur precursor is justified for controlling the nanoparticles growth once the formation of mono-sized nanocrystals is favoured by diffusion-limited growth. In this sense, the hydrolysis of thioacetamide is a way to manipulate the rate of nanoparticle growth reaction through the control of the concentration of reactant (Cao, 2004). For "SOL_TMC" used as ligand, the pH was adjusted to (11.5 ± 0.2) by addition of 0.1 mol L^{-1} sodium hydroxide solution.

On the other hand, sodium sulphides are readily available for quantum dots synthesis, despite de pH. The pH value of "SOL_CHI" solution was adjusted to (6.0 ± 0.2) (NaOH, 0.1 mol L^{-1}).

A typical synthesis was carried out as follows: 47 mL of "SOL_CHI" or "SOL_TMC" after pH adjustment were added to the flask reacting vessel. Under moderate magnetic stirring, 4.0 mL of cadmium precursor solution ($Cd(ClO_4)_2$, "SOL-Cd) and 2.5 mL of sulphur source solution (CH_3CSNH_2, "SOL_S1" or Na_2S, "SOL_S2")

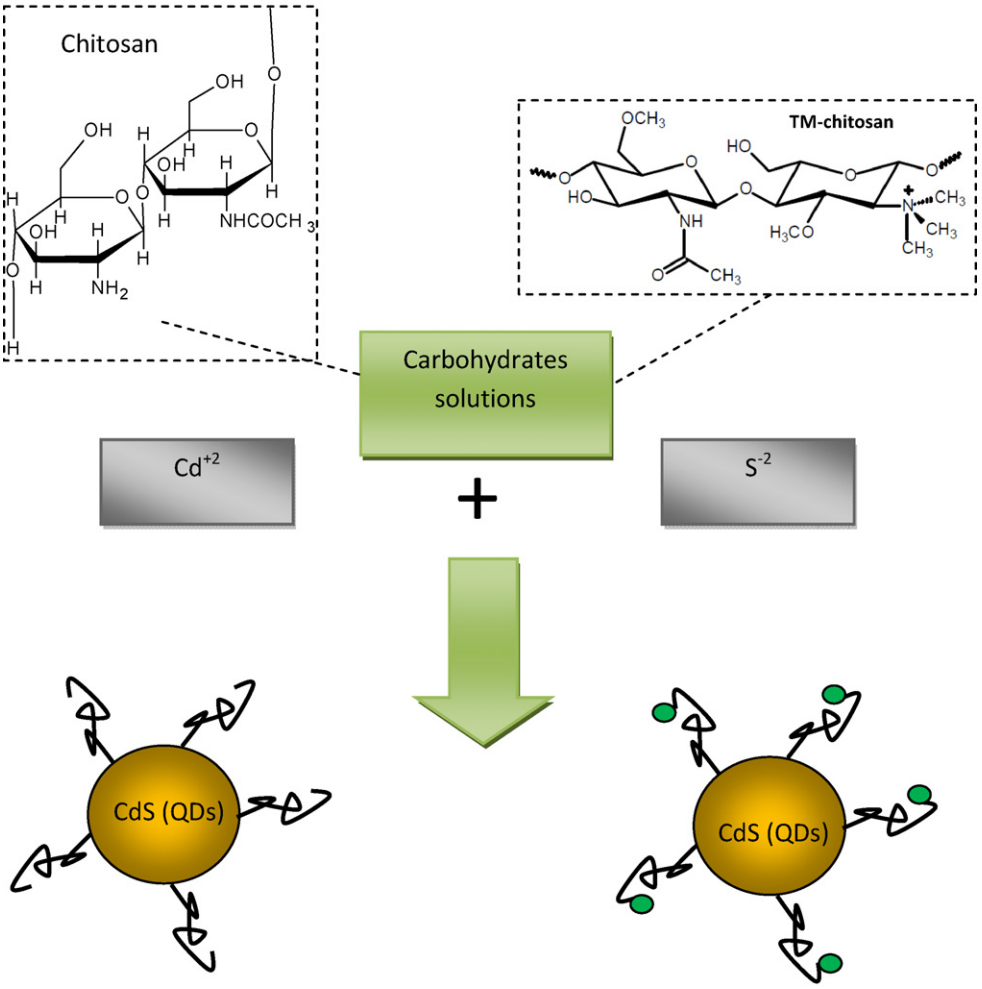

Fig. 1. Schematic representation of the designed experimental procedure for the CdS–carbohydrates colloidal system; molecular structures of chitosan and *N*,*N*,*N*-trimethylchitosan (TM-chitosan).

were added to the flask (S:Cd molar ratio was kept at 1:2). The solution turned yellowish and sampling aliquots of 3.0 mL were collected at different time intervals (after preparation, 1 day, 3 days, and 5 days) for UV–vis spectroscopy measurements that were used for kinetics analysis and colloidal stability evaluation.

In Fig. 1 it is shown the schematic representation of the experimental procedure performed for the synthesis of CdS-chitosan and CdS-TM-chitosan capped systems.

The simplified reactions of CdS synthesis using thioacetamide decomposition and sodium sulphide are represented in Eqs. (2) and (3), respectively:

$$Cd^{2+}{}_{(aq)} + CH_3C(S)NH_{2(aq)} + H_2O \rightarrow CdS_{(s)}\downarrow + CH_3C(O)NH_{2(aq)} + 2H^{+}{}_{(aq)} \quad (2)$$

$$Cd^{2+}{}_{(aq)} + S^{2-}{}_{(aq)} \rightarrow CdS\downarrow \quad (3)$$

2.6. Characterization of carbohydrates

The ^{1}H-NMR (Nuclear Magnetic Resonance) spectra of *N*,*N*,*N*-trimethyl chitosan was acquired at 80 °C in a 200 MHz Bruker AC200 spectrometer. For this analysis, the sample was dissolved in D_2O at a concentration of 10 g L^{-1}. The average degree of quaternization (DQ) was determined as previously described (Curti et al., 2003). The Fourier Transform Infrared (FTIR) spectrum of the sample was obtained in a Bomem FTIR 102 spectrometer, in the region of 4000–400 cm^{-1}. The Raman spectrum was performed on a Brucker RFS 100 machine equipped with a laser Nd^{+3}/YAG laser operating at 1064 nm in the near infrared and a CCD detector cooled with liquid nitrogen, spectral resolution of 4 cm^{-1}, an average of 600 accumulations and with power ranging from 200 to 300 mW.

2.7. Characterization of CdS quantum dots

UV–vis spectroscopy measurements were conducted using Perkin-Elmer equipment (Lambda EZ-210), wavelength from 600 nm to 190 nm, in transmission mode, using quartz cuvette. The absorption spectra were used to monitor the reaction for the formation of CdS QDs and their relative colloidal stability in the medium. Moreover, based on the "absorbance onset" of the curve it was possible to calculate the average nanoparticles sizes and their optical properties. All experiments were conducted in triplicates ($n = 3$) unless specifically noted. The statistical analysis (descriptive) of the set of data was performed assuming the mean ("central tendency") and the standard deviation ("dispersion") where needed. All experiments were conducted in triplicates ($n = 3$) unless specifically noted.

The emission spectra of the CdS nanocrystals were acquired by using Nanodrop^{TM} 3300 fluoro-spectrometer (Thermo Scientific). The excitation source comes from one of two solid-state light emitting diodes (LEDs): UV LED with $\lambda_{excitation} = (365 \pm 10)$ nm and Blue

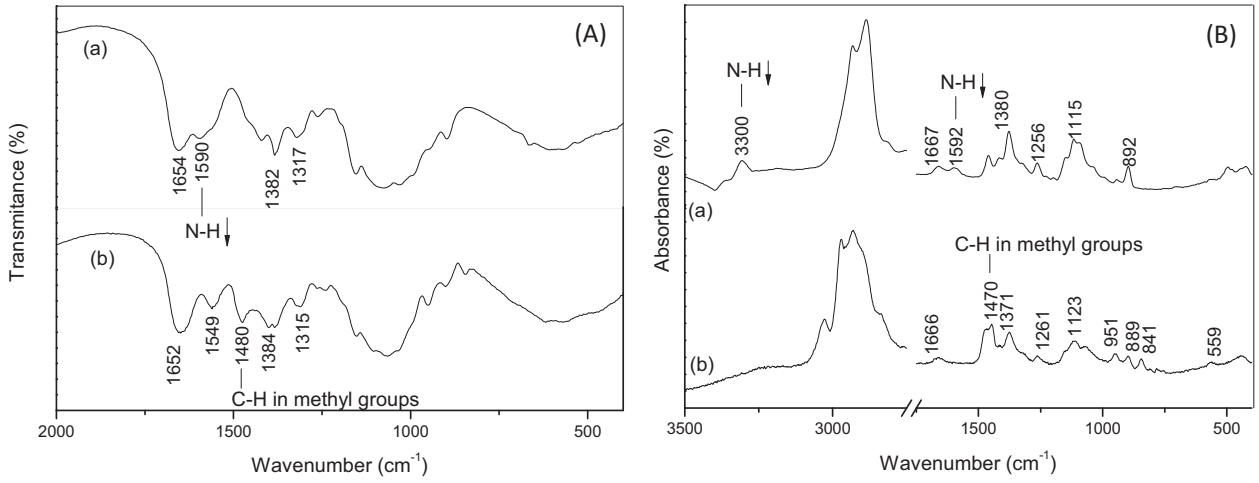

Fig. 2. (A) Infrared spectra and (B) Raman spectra of (a) chitosan (b) TM-chitosan.

LED with $\lambda_{excitation} = (470 \pm 10)$ nm. Both are equipped with cut filters that eliminate excitation above 400 nm (UV) or 495 nm (blue). All the photoluminescence (PL) spectra were collected at room temperature.

Measurement of fluorescence was reported in Relative Fluorescent Units (RFU) at the wavelength where the emission spectra reached its maximum intensity. The relative activity was calculated by subtracting the background of samples without the presence of QDs. All tests were performed using a minimum of four replicates ($n \geq 4$).

3. Results and discussion

3.1. Characterization of carbohydrates

The changes in the macromolecule of chitosan after the alkylation reaction can be observed by infrared spectroscopy. Unlike the spectrum of chitosan (Fig. 2A(a)) in the spectrum of alkylated sample (Fig. 2A(b)) is shown a characteristic band around 1480 cm^{-1} which is attributed to asymmetric angular deformation of methyl groups introduced into the polymer chain by *N*-alkylation (Martins, Pereira, Fajardo, Rubira, & Muniz, 2011). We can observe also that the band of NH in 1590 cm^{-1} decreases in intensity, which is due to methylation of amino groups (Martins et al., 2011).

The changes after alkylation of chitosan can also be observed in the Raman spectra (Fig. 2B). In the spectrum of the TM-chitosan (Fig. 2B(b)) was observed the absence of the bands at 3300 and 1590 cm^{-1} corresponding to the axial and angular deformation of NH, respectively, due to trimethylation of amino groups of chitosan. Comparing the spectrum of the TM-chitosan with the spectrum of chitosan we can observe that the band at 1470 cm^{-1} is much more intense due to the presence of methyl groups on the quaternized nitrogen atoms of TM-chitosan (Nazar et al., 2011).

The ^{1}H NMR spectrum of the sample of TM-chitosan is shown in Fig. 3. According to the literature (Sieval et al., 1998) the signal characteristic of quaternized site is located in the region of 3.3 ppm and the signal corresponding to the dimethylation of the amino group at 2.8 ppm. The hydrogen atom bonded to carbon 1 of the glucopyranose ring is responsible for the set of signals ranging from 4.5 to 5.5 ppm.

The average degree of quaternization (DQ) is the most important characteristic of *N*,*N*,*N*-trimethylchitosan. The ^{1}H NMR spectra are considered the best technique to evaluate the degree of quaternization of TM-chitosan (Curti et al., 2003). The area under the signals

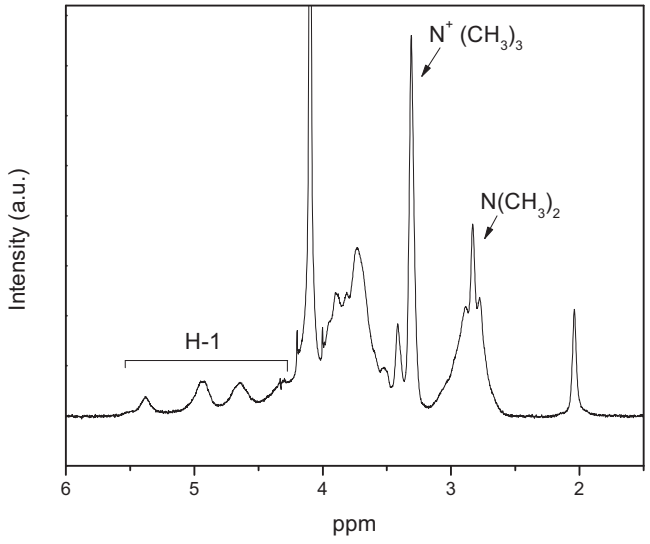

Fig. 3. ^{1}H NMR spectrum of the TM-chitosan dissolved in D_2O. (C_p = 10 g L^{-1}): pulse 90 and number of scans 16.

due to the hydrogen atom bonded to carbon 1 of the glucopyranose ring is taken as the reference signal. From the assignments mentioned above and taking into account the ratio between the area under the reference signal (A_{H1}) and that under the signals due to the hydrogen atoms of the methyl moieties of the trimethylated amino group (A_{CH_3}), it is possible to determine the average degree of quaternization (*DQ*) of the *N*,*N*,*N*-trimethylchitosan (Curti et al., 2003), by using Equation 4. Thus, the average degree of quaternization (DQ) of TM-chitosan sample was approximately 18%.

$$\%DQ = \left[\frac{A_{CH_3}}{9 \times A_{H1}}\right] \times 100 \quad (4)$$

3.2. Characterization of CdS quantum dots

Here, it is assumed some fundamental background on physics and chemistry of semiconductor nanocrystals. In short, due to their extreme small size, semiconductor nanoparticles with the dimensions below the so-called "Bohr-radius" will present a "quantum-confinement effect", related to the strong interaction between the pair "hole–electron" generated by exciting photon (Brus, 1984). It means that after reaching a specific threshold in

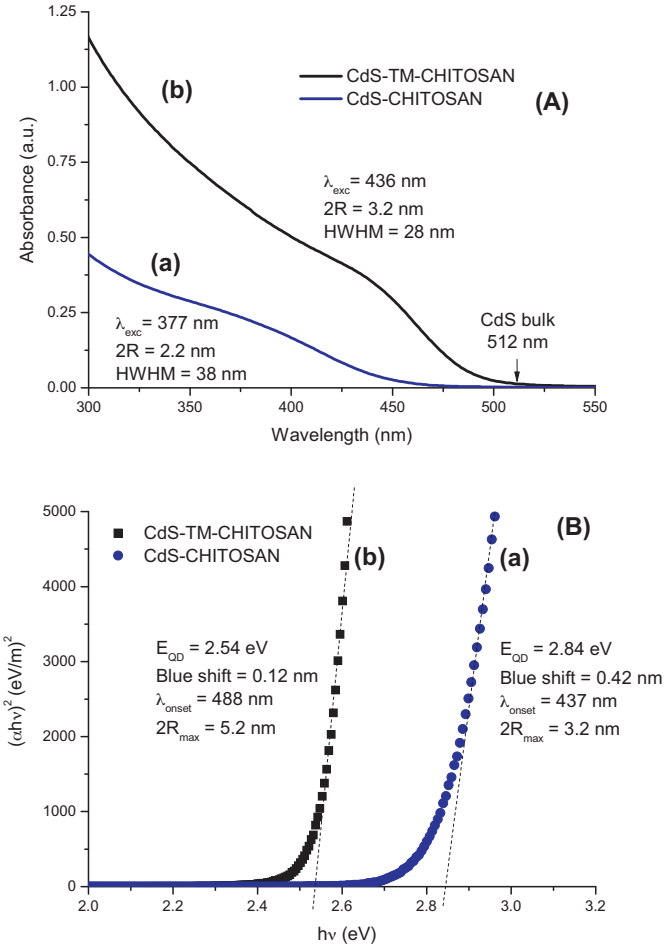

Fig. 4. (A) UV–vis absorption spectra and (B) optical absorption spectra of CdS nanoparticles in carbohydrates media after 5 days preparation: (a) chitosan; (b) TM-chitosan.

particle size (R = radius), the band gap is larger than that of the original bulk material (Mansur, 2010). As a consequence, through UV–vis spectroscopy method, the "absorbance onset" on the curve will be directly related to the altered band gap caused by the quantum-size effect.

Essentially, in this study, the average nanoparticle size was determined from Henglein's empirical model (Weller et al., 1986) which relates the CdS nanoparticle diameter ($2R$) to the optical "absorption onset" from UV–vis spectra. Nonetheless, the assessment of the optical band gap (E_{QD}) using the "Tauc relation" (Tauc & Menth, 1972; Winter, Gomez, Gatzert, Schmidt, & Korgel, 2005) has been acknowledged as a more precise method for obtaining the wavelength value (λ_{onset}) associated with the "absorbance onset". This procedure has been widely utilized for estimating average nanoparticles sizes directly from solutions via the UV–vis spectroscopy method.

In Fig. 4A, it is presented the UV–vis spectroscopy results from the synthesis of semiconductor nanoparticles using the carbohydrates as the stabilizing ligands. The CdS quantum dots were produced and stabilized with the carbohydrate-based ligands (after 5 days) with average size ($2R$), obtained from Henglein's empirical model and wavelength value of the first exciton (λ_{exc}), of (3.2 ± 0.1) nm and (2.2 ± 0.1) nm, using TM-chitosan and chitosan, respectively. Analogously, in Fig. 4B it can be observed that both CdS colloidal suspensions using chitosan and chemically modified chitosan were formed with the estimated average optical band gap of $E_{QD} = (2.84 \pm 0.02)$ eV and (2.54 ± 0.02) eV, respectively. These values are higher than the bulk value of 2.4 eV reported for CdS (Mansur, 2010), proving that quantum dots of CdS were successfully synthesized through this single-step route using carbohydrates as the capping moieties for the nanoparticles. The summary of results extracted from UV–vis spectra and optical absorbance analysis is presented in Table 1.

The half-width at half-maximum (HWHM) on the low energy side of the first exciton absorption peak position can be used as convenient index of size distribution (Dai et al., 2006). The smaller HWHM is corresponding to the narrower size distribution (Yu, Falkner, Shih, & Colvin, 2004). The HWHM of nanocrystals synthesized using organometallic precursors usually relays in the range of 10–20 nm (Dai et al., 2006; Yu, Qu, Guo, & Peng, 2003). Quantum dots prepared in aqueous solutions have a peak width quite broad (Yu, Wang, & Peng, 2003). The HWHM values were (28 ± 1) nm and (38 ± 1) nm for CdS-TM-chitosan and CdS-chitosan. It can be seen, as expected, that both parameters were broader than the typically obtained from non-aqueous routes. Also the quantum dots synthesized using thioacetamide as S^{2-} precursor have presented a smaller HWHM, which may be associated with the control of sulphur ions release by thioacetamide hydrolysis which favours diffusion-limited nanoparticle growth.

These findings can be discussed considering both thermodynamics and kinetics aspects associated with colloidal chemistry. That means, the reaction of Cd^{2+} with S^{2-} in water medium producing CdS crystals is very favourable ($\Delta G < 0$). Besides, regarding to the kinetics, the reaction rate is determined by the extremely small value of the "solubility product constant" ($K_{sp} = 8.0 \times 10^{-27}$). On the other hand, the just nucleated nanocrystals would tend to behave like "seeds" for further growth or promoting some agglomeration driven by the reduction in surface energy, i.e. by decreasing the surface area (S) to volume (V) ratio (Mansur & Mansur, 2011; Mansur, H. S., et al., 2011a). Therefore, in order to stabilize the formed CdS quantum dots in the aqueous solution, an effective capping agent must to be utilized. Hence, in the present study, the results have showed that chitosan and chitosan-derivative (TM-chitosan) were remarkably effective as ligands for stabilizing the colloidal semiconductor quantum dots in aqueous media. Nevertheless, TM-chitosan would be the main choice considering biomedical applications as it is water-soluble under physiological conditions ($6.5 < pH < 7.5$; Kellum, 2000). Despite being beyond the focus of this research, apparently, the most probable mechanism acting on the system is the reduction of the surface energy of the CdS QDs by the interactions of the chemical groups from carbohydrates chains, as schematically represented in Fig. 5. Due to the "excess" of cadmium ions compared to sulphides in the synthesis, $[Cd^{2+}]/[S^{2-}] = 2:1$, it is expected to have stabilization by electronegative groups, like amino and hydroxyl groups presents in chitosan polymeric chains. This assumption is endorsed by the relative smaller size for CdS QDs synthesized with chitosan (~2.2 nm) compared to chemically modified chitosan (~3.2 nm). That means, the chemical functionalization performed in the chitosan polymer (TM-chitosan) have introduced positively charged moieties raising repulsive forces to the Cd^{2+} at the QDs surfaces combined to the steric hindrance due to the presence of methyl groups on the quaternized nitrogen atoms of the carbohydrate chains. Moreover, chitosan and chitosan-derivatives are very pH-dependent causing differences in the macromolecules charge profiles. These effects have significantly reduced the capping behaviour of TM-chitosan onto the CdS QDs surfaces. It should be emphasized that it is a simplified approach for the developed system. Obviously, several other interactions were present in this complex nano-hybrid system, such as hydrophilic and hydrophobic interactions, hydrogen bonds, steric hindrance among polymer chains (3D conformation). Therefore, a deeper understanding of the adsorption phenomenon

Table 1
Quantum dots parameters: band-gap energy, blue-shift, estimated particle size.

System	S^{2-} precursor	pH	Parameter	After preparation	5 days
CdS-TM-chitosan	Thioacetamide	11.5 ± 0.2	Band gap (eV)	2.52 ± 0.02	2.54 ± 0.02
			Blue shift (eV)	0.10 ± 0.02	0.12 ± 0.02
			λ_{onset} (nm)	492 ± 2	488 ± 2
			$2R_{max}$ (nm)	5.4 ± 0.1	5.2 ± 0.1
			λ_{exc} (nm)	434 ± 2	436 ± 2
			$2R$ (nm)	3.1 ± 0.1	3.2 ± 0.1
			HWHM	30 ± 1	28 ± 1
CdS-chitosan	Sodium sulphide	6.0 ± 0.2	Band gap (eV)	2.80 ± 0.02	2.84 ± 0.02
			Blue shift (eV)	0.38 ± 0.02	0.42 ± 0.02
			λ_{onset} (nm)	443 ± 2	437 ± 2
			$2R_{max}$ (nm)	3.3 ± 0.1	3.2 ± 0.1
			λ_{exc} (nm)	378 ± 2	377 ± 2
			$2R$ (nm)	2.2 ± 0.1	2.2 ± 0.1
			HWHM	37 ± 1	38 ± 1

Error bar = one standard deviation.

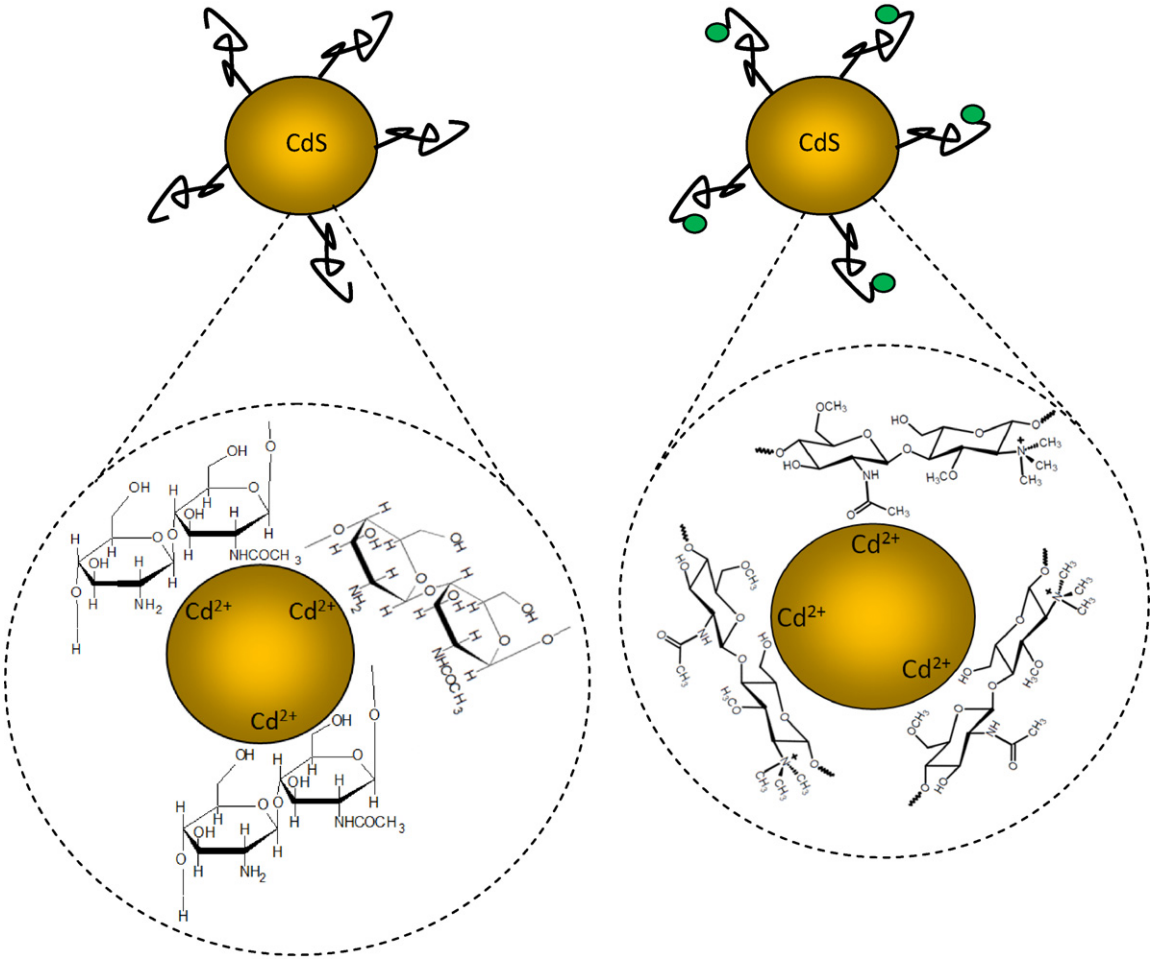

Fig. 5. Schematic representation of the mechanism of interactions between the CdS quantum dots and the chemical groups from carbohydrates chains (chitosan, left; TM-chitosan, right).

must take into account the entire balance of forces involved at the interface of quantum dot/polymer ligand (Mansur & Mansur, 2011; Mansur, H. S., et al., 2011a; Nel et al., 2009).

While the optical absorption spectroscopy reflects the band structure of synthesized materials, fluorescence spectroscopy gives information on the trap states of the particles. Occurrence, population, and depths of the traps determine if the electron–hole pair generated by the absorption of light will recombine under the emission of light and/or nonradiatively.

It has been reported that crystals of CdS have luminescence in blue, green, orange, and red regions of spectra (Mansur, A., et al., 2011; Smyntyna, Skobeeva, & Malushin, 2007). Blue luminescence is associated with the excitonic emission and it is represented by discrete narrow lines or it is not observed at all (Smyntyna et al., 2007). In the green spectra region, a band at 515 nm up to 522 nm is detected CdS nanoparticles. According to the literature, it is favoured by the synthesis of the nanoparticles under the condition of excess of atoms of the metal that enter in the

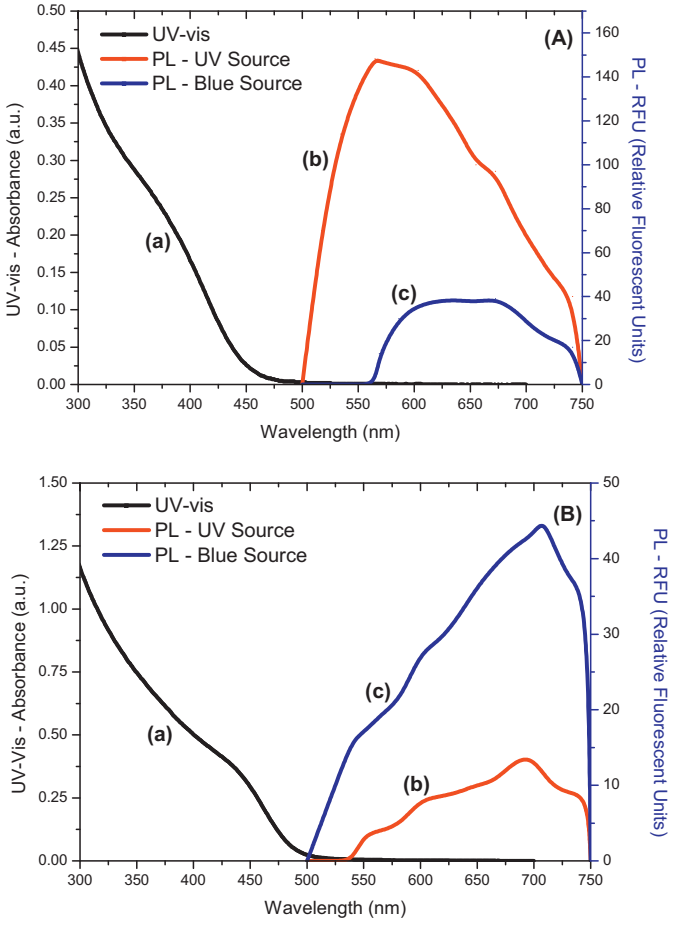

Fig. 6. UV–vis spectra (a) and PL ((b) UV LED and (c) blue LED) spectra obtained from (A) CdS-chitosan and (B) CdS-TM-chitosan.

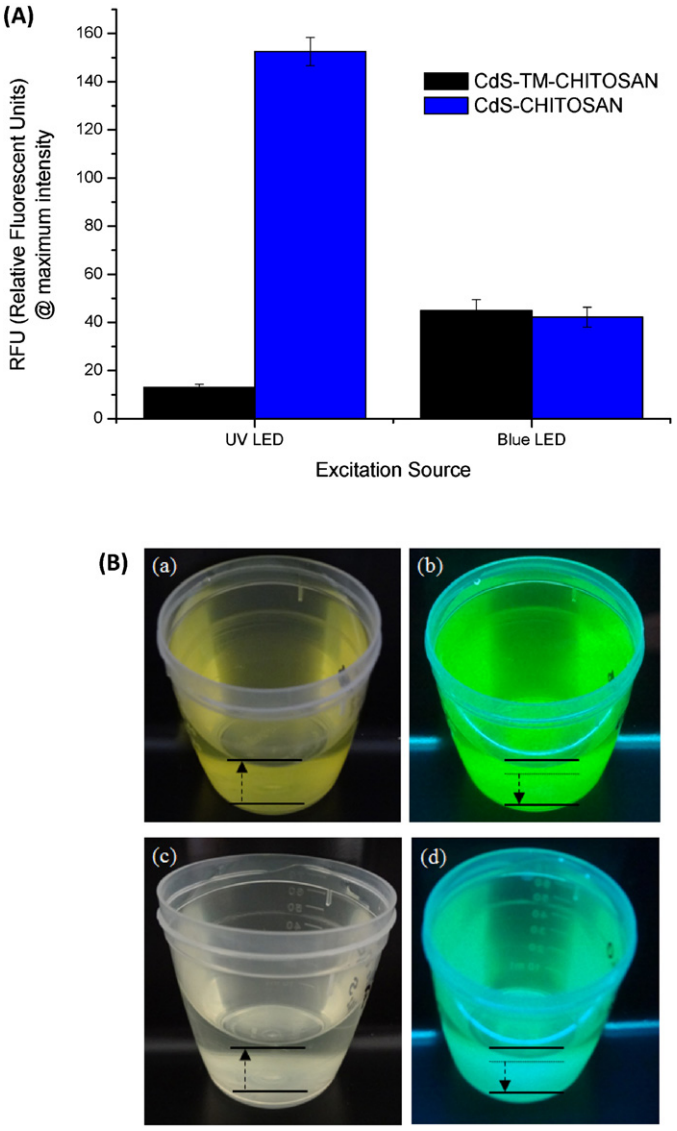

Fig. 7. (A) Intensity of fluorescence obtained of CdS-TM-chitosan and CdS-chitosan for excitation wavelengths 365 nm (UV) and 470 nm (blue). (B) Quantum dot solutions under natural light illumination ((a) for CdS-TM-chitosan and (c) for CdS-CHI) and fluorescing under 245 nm UV irradiation ((b) for CdS-TM-chitosan and (d) for CdS-CHI).

lattice at interstitial sites (Cd_i) (Lakowicz, Gryczynski, Gregorz, & Murphy, 2002; Smyntyna et al., 2007) or it is attributed to interstitial sulphur (S_i) formed through substitutional doping of CdS by anions like Cl^- (Ramsden & Gratzel, 1984). Orange luminescence (590–625 nm) is observed in the case when interstitial atoms of metal are present in the lattice of semiconductor and red band of PL is typically observed in the nanoparticles which contain a certain concentration of intrinsic defects of the type $V_{Cd} - V_s$ (di-vacancies) (Smyntyna et al., 2007) or V_s (Ramsden & Gratzel, 1984).

The fluorescence spectra of CdS nanoparticles stabilized with chitosan and TM-chitosan are shown in Fig. 6A and B, respectively. The correspondent absorption spectra are also shown. CdS-chitosan and CdS-TM-chitosan nanocrystals exhibit broadband emission (500–750 nm) that covers most of the visible spectrum ("white band"). Their luminescence originates from states that are much lower in energy than the absorbing state being associated with deep trap states. The observed wide band is associated with some of the emissions of CdS described in the previous paragraph that are overlapped.

It should also be highlighted that the quantum dots stabilizers present primary, secondary and quaternary (TM-chitosan) amino groups in their structures. Amines could act as hole scavengers which quench photoluminescence or, when they attach onto quantum dots surfaces, due to the passivation of dangling bonds, they could increase the quantum yield despite their holes scavenging properties in solution (Baker & Kamat, 2010; Kalyuzhny & Murray, 2005; Landes, Braun, & El-Sayed, 2011). Based on that, the PL spectra also might reflect the overall balance of amine effect in quantum dots trap states, emission bands, and intensity. Fig. 7A shows the intensity at the maximum peak of PL curves (CdS-TM-chitosan: 690 nm for UV LED and 700 for blue LED; CdS-CHI: 565 nm for UV LED and 671 for blue LED) for CdS-TM-chitosan and CdS-chitosan indicating their fluorescent activity. The digital images taken from the colloidal bioconjugates (CdS–ligand) are presented in Fig. 7. The quantum dots systems with natural light illumination (no magnification) and under UV–vis excitation (fluorescence) are shown in Fig. 7B(a and c) and Fig. 7B(b and d), respectively.

4. Conclusions

It can be summarized that in the present study an aqueous colloidal route for producing CdS quantum dots was successfully developed using both chitosan and chemically modified chitosan as biopolymer-capping agents. Furthermore, they have shown some photoactivity fairly suitable for potential use as fluorescent biomarkers for innumerous applications such as biomedical labelling, imaging, and biosensing. In that sense, these novel carbohydrate-based nanohybrids pave the way for combining

biomacromolecules and inorganic semiconductor quantum dots specially tailored to be explored in nanomedicine research.

Acknowledgements

The authors acknowledge the financial support from CAPES, FAPEMIG and CNPq.

References

Baker, D. R., & Kamat, P. V. (2010). Tuning the emission of CdSe quantum dots by controlled trap enhancement. *Langmuir*, *26*, 11272–11276.

Brus, L. E. (1984). Electron–electron–hole in small semiconductors crystallites: The size dependence of the lowest excited electronic state. *The Journal of Chemical Physics*, *80*, 4403–4409.

Cao, G. (2004). *Nanostructures and nanomaterials: Synthesis, properties and applications*. London: Imperial College Press.

Costa-Júnior, E. S., Barbosa-Stancioli, E. F., Mansur, A. A. P., Vasconcelos, W. L., & Mansur, H. S. (2009). Preparation and characterization of chitosanpoly(vinyl alcohol) chemically crosslinked blends for biomedical applications. *Carbohydrate Polymers*, *76*, 472–481.

Curti, E., Britto, D., & Campana-Filho, S. P. (2003). Methylation of chitosan with iodomethane: Effect of reaction conditions on chemoselectivity and degree of substitution. *Macromolecular Bioscience*, *3*, 571–576.

Dai, Q., Li, D., Jiang, S., Chen, H., Wang, Y., Kan, S., et al. (2006). Synthesis of monodisperse CdSe nanocrystals directly to air: Monomer reactivity tuned by the selenium ligand. *Journal of Crystal Growth*, *292*, 14–18.

Dash, M., Chiellini, F., Ottenbrite, R. M., & Chiellini, E. (2011). Chitosan-A versatile semi-synthetic polymer in biomedical applications. *Progress in Polymer Science*, *36*, 981–1014.

Dutta, P. K., Dutta, J., & Tripathi, V. S. (2004). Chitin and chitosan: Chemistry, properties and applications. *Journal of Scientific and Industrial Research*, *63*, 20–31.

Jiang, R., Zhu, H., Yao, J., Fu, Y., & Guan, Y. (2012). Chitosan hydrogel films as a template for mild biosynthesis of CdS quantum dots with highly efficient photocatalytic activity. *Applied Surface Science*, *258*, 3513–3518.

Kalyuzhny, G., & Murray, R. W. (2005). Ligand effects on the optical properties of CdSe nanocrystals. *The Journal of Physical Chemistry B*, *109*, 7012–7021.

Kellum, J. A. (2000). Determinants of blood pH in health and disease. *Critical Care*, *4*, 6–14.

Lakowicz, J., Gryczynski, I., Gregorz, P., & Murphy, C. (2002). Emission spectral properties of cadmium sulfide nanoparticles with multiphonon excitation. *The Journal of Physical Chemistry B*, *106*, 5365–5370.

Landes, C. F., Braun, M., & El-Sayed, M. A. (2011). On the nanoparticle to molecular size transition: Fluorescence quenching studies. *The Journal of Physical Chemistry B*, *105*, 10554–10558.

Li, Z., Du, Y., Zhang, Z., & Pang, D. (2003). Preparation and characterization of CdS quantum dots chitosan biocomposite. *Reactive and Functional Polymers*, *55*, 35–43.

Li, Y. C., Zhong, H. Z., Zhou, Y., Yang, C. H., & Li, Y. F. (2006). High-yield fabrication and electrochemical characterization of tetrapodal CdSe, CdTe, and $CdSe_xTe_{1-x}$ nanocrystals. *Advanced Functional Materials*, *16*, 1705–1716.

Mansur, H. S. (2010). Quantum dots and nanocomposites. *Wiley International Reviews: Nanomedicine and Nanobiotechnology*, *2*, 113–129.

Mansur, H. S., Grieser, F., Marychurch, M. S., Biggs, S., Urquhart, R. S., & Furlong, D. N. (1995). Photoelectrochemical properties of Q-state CDS particles in arachidic acid Langmuir–Blodgett-films. *Journal of the Chemical Society, Faraday Transactions*, *91*, 665–672.

Mansur, H. S., Grieser, F., Urquhart, R. S., & Furlong, D. N. (1995). Photoelectrochemical behaviour of Q-state $CdS_xSe_{(1-x)}$ particles in arachidic acid Langmuir–Blodgett films. *Journal of the Chemical Society, Faraday Transactions*, *91*, 3399–3404.

Mansur, H. S., & Mansur, A. A. P. (2011). CdSe quantum dots stabilized by carboxylic-functionalized PVA: Synthesis and UV–vis spectroscopy characterization. *Materials Chemistry and Physics*, *125*, 709–717.

Mansur, H. S., & Mansur, A. A. P. (2012). Fluorescent nanohybrids: Quantum-dots coupled to polymer-recombinant protein conjugates for the recognition of biological hazards. *Journal of Materials Chemistry*, *22*, 9006–9018.

Mansur, A., Mansur, H., & González, J. (2011). Enzyme–polymers conjugated to quantum-dots for sensing applications. *Sensors*, *11*, 9951–9972.

Mansur, H. S., Mansur, A. A. P., & González, J. C. (2011a). Biomolecule-quantum dot systems for bioconjugation applications. *Colloids and Surfaces B: Biointerfaces*, *84*, 360–368.

Mansur, H. S., Mansur, A. A. P., & González, J. C. (2011b). Synthesis and characterization of CdS quantum dots with carboxylic-functionalized poly (vinyl alcohol) for bioconjugation. *Polymer*, *52*, 1045–1054.

Martins, A. F., Pereira, A. G. B., Fajardo, A. R., Rubira, A. F., & Muniz, E. C. (2011). Characterization of polyelectrolytes complexes based on *N*,*N*,*N*-trimethyl chitosan/heparin prepared at different pH conditions. *Carbohydrate Polymers*, *86*, 1266–1272.

Mansur, H. S., Vasconcelos, W. L., Grieser, F., & Caruso, F. (1999). Photoelectrochemical behavior of CdS Q-state semiconductor particles in 10,12 nonacosadiynoic acid polymer LB film. *Journal of Materials Science*, *34*, 5285–5291.

Medintz, I. L., Uyeda, H. T., Goldman, E. R., & Mattoussi, H. (2005). Quantum dot bioconjugates for imaging, labelling and sensing. *Nature Materials*, *4*, 435–446.

Muzzarelli, R. A. A. (2009). Chitins and chitosans for the repair of wounded skin, nerve, cartilage and bone. *Carbohydrate Polymers*, *76*, 167–182.

Muzzarelli, R. A. A. (2011). Chitosan composites with inorganics, morphogenetic proteins and stem cells, for bone regeneration. *Carbohydrate Polymers*, *83*, 1433–1445.

Muzzarelli, R. A. A., Boudrant, J., Meyer, D., Manno, N., DeMarchis, M., & Paoletti, M. G. (2012). Current views on fungal chitin/chitosan, human chitinases, food preservation, glucans, pectins and inulin: A tribute to Henri Braconnot, precursor of the carbohydrate polymers science, on the chitin bicentennial. *Carbohydrate Polymers*, *87*, 995–1012.

Nazar, H., Fatouros, D. G., van der Merwe, S. M., Bouropoulos, N., Avgouropoulos, G., Tsibouklis, J., et al. (2011). Thermosensitive hydrogels for nasal drug delivery: The formulation and characterisation of systems based on *N*-trimethyl chitosan chloride. *European Journal of Pharmaceutics and Biopharmaceutics*, *77*, 225–232.

Nel, A. E., Mädler, L., Velegol, D., Xia, T., Hoek, E. M. V., Somasundaran, P., et al. (2009). Understanding biophysicochemical interactions at the nano–bio interface. *Nature Materials*, *8*, 543–557.

Peeters, O. M., & de Ranter, C. J. (1974). Pathways in thioacetamide hydrolysis in aqueous acid: Detection by kinetic analysis. *Journal of the Chemical Society, Perkin Transactions*, *2*, 1832–1835.

Ramsden, J. J., & Gratzel, M. (1984). Photoluminescence of small cadmium sulphide particles. *Journal of the Chemical Society, Faraday Transactions*, *80*, 919–933.

Rinaudo, M. (2006). Chitin and chitosan: Properties and applications. *Progress in Polymer Science*, *31*, 603–632.

Rosenthal, D., & Taylor, T. I. (1957). A study of the mechanism and kinetics of the thioacetamide hydrolysis reaction. *Journal of the American Chemical Society*, *79*, 2684–2690.

Sieval, A. B., Thanou, M., Kotzé, A. F., Verhoef, J. C., Brussee, J., & Junginger, H. E. (1998). Preparation and NMR characterization of highly substituted *N*-trimethyl chitosan chloride. *Carbohydrate Polymers*, *36*, 157–165.

Smyntyna, V., Skobeeva, V., & Malushin, N. (2007). The nature of emission centers in CdS nanocrystals. *Radiation Measurements*, *42*, 693–696.

Tauc, J., & Menth, A. (1972). States in the gap. *Journal of the Non-Crystalline Solids*, *8–10*, 569–585.

Urquhart, R. S., Furlong, D. N., Mansur, H. S., Grieser, F., & Tanaka, K. (1994). Quartz crystal microbalance and UV–vis absorption study of Q-state particles in arachidic acid LB films. *Langmuir*, *10*, 899–902.

Weller, H., Schmidt, H. M., Koch, U., Fojtik, A., Baral, S., Henglein, A., et al. (1986). Photochemistry of colloidal semiconductors. Onset of light absorption as a function of size of extreme small CdS particles. *Chemical Physics Letters*, *124*, 557–560.

Winter, J. O., Gomez, N., Gatzert, S., Schmidt, C. E., & Korgel, B. A. (2005). Variation of cadmium sulfide nanoparticles size and photoluminescence intensity with altered aqueous synthesis conditions. *Colloids and Surfaces A: Physicochemical and Engineering Aspects*, *254*, 147–157.

Ye, M., Zhong, H., Zheng, W., Yang, C., & Li, Y. (2007). Ultralong cadmium hydroxide nanowires: Synthesis, characterization and transformation into CdO nanostrands. *Langmuir*, *23*, 9064–9068.

Yu, W. W., Falkner, J. C., Shih, B. S., & Colvin, V. L. (2004). Preparation and characterization of monodisperse PbSe semiconductor nanocrystals in a noncoordinating solvent. *Chemistry of Materials*, *16*, 3318–3322.

Yu, W. W., Qu, L., Guo, W., & Peng, X. (2003). Experimental determination of the extinction coefficient of CdTe, CdSe, and CdS nanocrystals. *Chemistry of Materials*, *15*, 2854–2860.

Yu, W. W., Wang, Y. A., & Peng, X. (2003). Formation and stability of size-, shape-, and structure-controlled CdTe nanocrystals: Ligand effects on monomers and nanocrystals. *Chemistry of Materials*, *15*, 4300–4308.